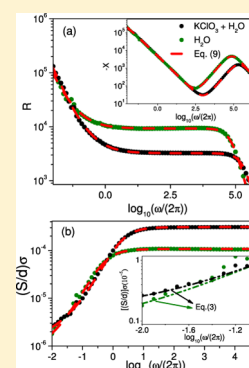


Ion Motion in Electrolytic Cells: Anomalous Diffusion Evidences

E. K. Lenzi,[†] R. S. Zola,^{‡,§} H. V. Ribeiro,[‡] Denner S. Vieira,[‡] F. Ciuchi,^{||} A. Mazzulla,^{||} N. Scaramuzza,^{||,⊥} and L. R. Evangelista^{*,‡,§}[†]Departamento de Física, Universidade Estadual de Ponta Grossa, 87030-900 Ponta Grossa, Paraná, Brazil[‡]Departamento de Física, Universidade Estadual de Maringá, Avenida Colombo, 5790, 87020-900 Maringá, Paraná, Brazil[§]Departamento de Física, Universidade Tecnológica Federal do Paraná, Rua Marçílio Dias, 635, 86812-460 Apucarana, Paraná, Brazil^{||}CNR-NANOTEC sede di Rende, Licryl Laboratory, and Centro di Eccellenza CEMIF.CAL and [⊥]Dipartimento di Fisica, Università della Calabria, 87036 Arcavacata di Rende, Italy

ABSTRACT: In this study, we argue that ion motion in electrolytic cells containing Milli-Q water, weak electrolytes, or liquid crystals may exhibit unusual diffusive regimes that deviate from the expected behavior, leading the system to present an anomalous diffusion. Our arguments lie on the investigation of the electrical conductivity and its relationship with the mean square displacement, which may be used to characterize the ionic motion. In our analysis, the Poisson–Nernst–Planck diffusional model is used with extended boundary conditions to simulate the charge transfer, accumulation, and/or adsorption–desorption at the electrode surfaces.



INTRODUCTION

The very irregular state of motion observed by Robert Brown for small pollen grains suspended in water initiated one of the most fascinating fields of science. The importance of such discovery, the so-called diffusion process, is immeasurable, and it has been found in several contexts of nature. Satisfactory explanations for this motion were proposed by Einstein,¹ von Smoluchowski,² and Langevin³ in their pioneering works. The main feature of this random motion is the linear growth with time exhibited by the mean square displacement, that is, $\langle(\Delta z)^2\rangle \sim t$, which is characteristic of a Markovian process. In contrast with this situation, for example, living cells,⁴ crowding systems,^{5,6} and amorphous conductor⁷ all present a diffusion process that may exhibit a nonlinear time dependence for $\langle(\Delta z)^2\rangle$, typical of non-Markovian processes. This feature has implications on the physical properties of these systems, particularly on the electrochemical properties, which represent a relevant research field of material science. In this regard, an important scenario concerns the ion motion in disordered solids that may undergo a subdiffusive regime, indicating that the ionic motion is not random or temporally correlated.^{8–10} Among the possible implications on the physicochemical properties, the electrical conductivity of a material is directly influenced by the diffusion process.¹¹ One system for which an unusual behavior of the conductivity may be associated with an anomalous behavior of the diffusion regime is encountered in bent-core liquid crystals (LCs). For these materials, distinct conductivity spectra are commonly observed, which often switch sign (anisotropy) and can be associated to geometrical constraints inherent of the phase, such as the presence of

cybotactic clusters.^{12–14} In fact, the electrical conductivity may exhibit an unusual dependence on the frequency, for example, $\sigma(\omega) \sim \omega^\delta$ with $0 \leq \delta < 1$,⁸ leading to $\langle(\Delta z)^2\rangle \equiv \langle(z - \langle z \rangle)^2\rangle \propto t^{1-\delta}$, a typical characteristic of an anomalous diffusion. This result bridges the gap between an electrical measurement and the phenomenological descriptions of ionic motion. It also evidences that the electrical data obtained may be used to better understand the contributions of the bulk and surface effects to the ionic dynamics in different experimental scenarios.

Here, we analyze the relationship between the electrical conductivity and the ionic motion in Milli-Q water, weak electrolytes, and LCs in contact with different kinds of electrodes from the experimental data obtained via electrical impedance spectroscopy, shown in Figure 1. We establish the contribution of the surface and bulk effects to the diffusive regimes present in these systems by considering the relationship between the impedance, $Z(\omega)$, and the conductivity, $\sigma(\omega)$, thus enabling the use of Einstein's generalized relation between mobility $\mu(\omega)$ and diffusion constant to nonzero frequency $D(\omega)$, where $\mu(\omega) \propto D(\omega)$ and $\mu(\omega) \propto \sigma(\omega)$. Thus, we may obtain $D(\omega)$ and relate it to the mean square displacement that characterizes the diffusive process. We also use the Poisson–Nernst–Planck (PNP) model to relate the behavior of the conductivity to the contribution of the surface and/or the bulk depending on the frequency range.

Received: February 3, 2017

Revised: March 5, 2017

Published: March 15, 2017

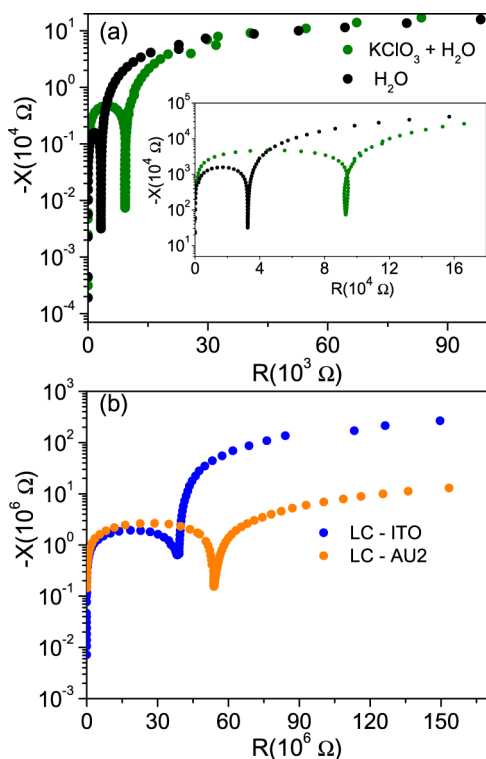


Figure 1. (a) Imaginary (X ($X = \text{Im } Z$)) vs real (R ($R = \text{Re } Z$)) parts of the impedance (Nyquist diagram) for the experimental data obtained from a weak electrolyte of KClO_3 (black circles) and Milli-Q water (green circles) (see ref 18 for more details on the experimental setup). (b) Experimental data obtained from electrolytic cell with LCs by taking into account electrodes with gold pixel on the surface (LC-Au) (orange circles) and electrodes made of indium tin oxide (ITO) (blue circles) (see ref 19 for more details on the experimental setup).

THEORY

The PNP model is based on the continuity equation, $\partial_t n_{\pm}(z, t) + \partial_z j_{\pm}(z, t) = 0$, in relation to the current density

$$j_{\pm}(z, t) = -D_{\pm} \frac{\partial}{\partial z} n_{\pm}(z, t) \mp \frac{qD_{\pm}}{k_B T} n_{\pm}(z, t) \frac{\partial V(z, t)}{\partial z} \quad (1)$$

where $D_+ = D_- = D$ is the diffusion coefficient (the same for positive and negative ions), $V(z, t)$ is the effective electric potential across the sample of thickness d , k_B is the Boltzmann constant, T is the absolute temperature, q is the effective charge, and $n_{\pm}(z, t)$ is the density of ions across the sample. Furthermore, the potential $V(z, t)$ satisfies the Poisson equation, $\partial_z^2 V(z, t) = -q[n_+(z, t) - n_-(z, t)]/\epsilon$, where ϵ is the dielectric coefficient of the medium (measured in ϵ_0 units). We also consider it subjected to the boundary conditions^{15–20}

$$j_{\pm}(\pm d/2, t) = \pm \int_0^1 d\bar{\delta} \int_{-\infty}^t dt' \kappa(t - t', \bar{\delta}) \partial_t^{\bar{\delta}} n_{\pm}(\pm d/2, t') \quad (2)$$

where $\kappa(t, \bar{\delta})$ is a kernel convoluted with a fractional time derivative that can be related to the surface effects presented, such as adsorption–desorption¹⁵ and charge transfer.²¹ Equation 2 embodies several situations and leads to a scenario characterized by anomalous diffusion, as discussed in refs 22–24. In particular, it is worth mentioning that for $\kappa(t, \bar{\delta}) = \kappa e^{-t/\tau} \delta(\bar{\delta} - 1)$ the previous boundary conditions may account for an adsorption–desorption process at the surface governed

by a kinetic equation corresponding to the Langmuir approximation,²⁵ whereas for $\kappa(t, \bar{\delta}) = \kappa \delta(t) \delta(\bar{\delta})$, a Chang–Jaffé-like boundary condition is reobtained.²¹

RESULTS AND DISCUSSION

Let us now use the impedance obtained by solving the previous equations (see Appendix for details) with $\bar{\kappa}(i\omega) = \bar{\kappa}_1(i\omega)^{\delta_1} + \bar{\kappa}_2(i\omega)^{\delta_2}$ to investigate the experimental data of Figure 1. It is worth mentioning that depending on the values of δ_1 and δ_2 , $\bar{\kappa}(i\omega)$ may lead to a charge-transfer behavior and/or a capacitive-like behavior, which may be attributed to an accumulation and/or an adsorption–desorption process on the electrode surfaces. Figure 2a shows a comparison between

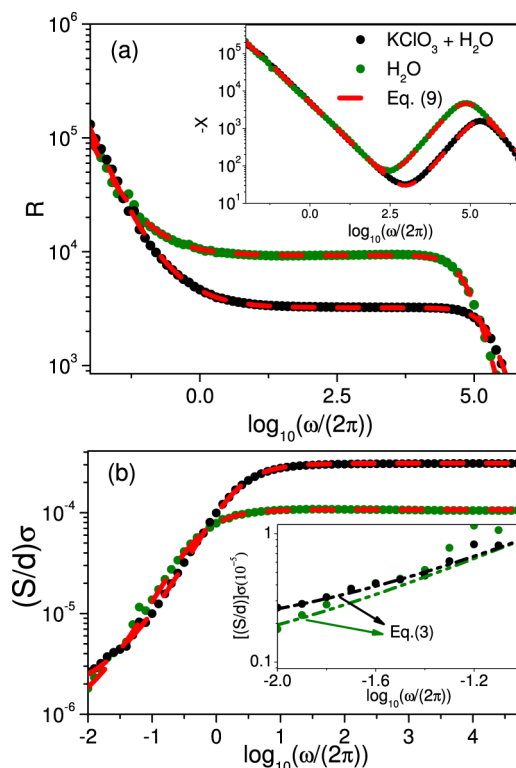


Figure 2. (a) Real part ($R = \text{Re } Z$) part vs $\log_{10}(\omega/2\pi)$; (b) scaled conductivity ($\sigma(S/d)$) vs $\log_{10}(\omega/2\pi)$. The inset in (a) shows imaginary part ($X = \text{Im } Z$) vs $\log_{10}(\omega/2\pi)$, and that in (b) shows the behavior of the conductivity in the low-frequency regime. The experimental data of KClO_3 (black circles), Milli-Q water (green circles), and eq 9 (red dotted line) are also shown. Note that the best agreement between the experimental data and the theoretical model is obtained for the case eq 9. For the electrolytic cell with KClO_3 , we used $D \approx 2.85 \times 10^{-9} \text{ m}^2 \text{ s}^{-1}$, $\lambda \approx 4.5 \times 10^{-8} \text{ m}$, $\epsilon \approx 82.0\epsilon_0$, $S = 3.14 \times 10^{-4} \text{ m}^2$, $d = 10^{-3} \text{ m}$, $\bar{\kappa}_2 = 7.0 \times 10^{-7} \text{ m s}^{-1+\delta_2}$, $\delta_2 = 0.83$, and $\bar{\kappa}_1 = 2.6 \times 10^{-8} \text{ m s}^{-1}$. For the case with Milli-Q water, we used $D \approx 3.4 \times 10^{-9} \text{ m}^2 \text{ s}^{-1}$, $\lambda \approx 8.38 \times 10^{-8} \text{ m}$, $\epsilon \approx 80.0\epsilon_0$, $S = 3.14 \times 10^{-4} \text{ m}^2$, $d = 10^{-3} \text{ m}$, $\bar{\kappa}_2 = 2.5 \times 10^{-5} \text{ m s}^{-1+\delta_2}$, $\delta_2 = 0.84$, and $\bar{\kappa}_1 = 4.3 \times 10^{-8} \text{ m s}^{-1}$.

this model (eq 9) and the experimental data obtained for a solution of KClO_3 and Milli-Q water, where an excellent agreement is observed. By using the same parameters, we show that the conductivity for these systems is also in good agreement with that of the model (see Figure 2b). In Figure 3, the experimental data obtained from the electrolytic cells with a LC (see ref 19 for more details) are compared with eq 9 and an excellent agreement is obtained. For this case, we also present the behavior of the conductivity and the model. The

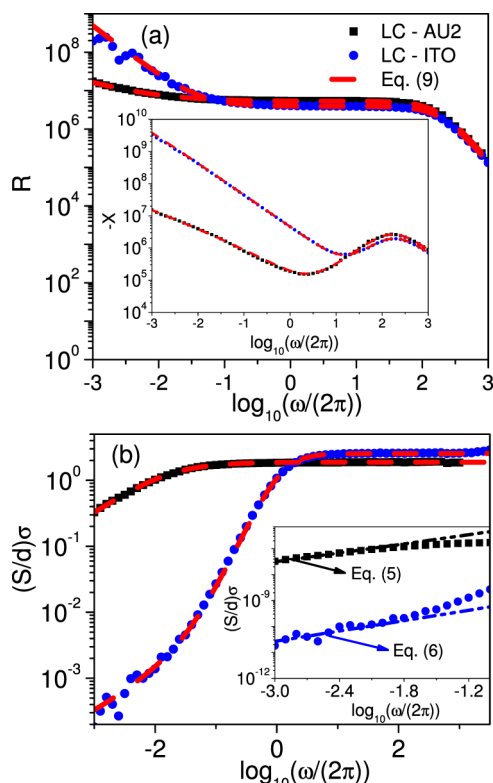


Figure 3. (a) Real part ($R = \text{Re } Z$) vs $\log_{10}(\omega/2\pi)$; (b) scaled conductivity ($\sigma(S/d)$) vs $\log_{10}(\omega/2\pi)$. The inset in (a) shows imaginary part ($X = \text{Im } Z$) vs $\log_{10}(\omega/2\pi)$, and that in (b) shows the behavior of the conductivity in the low-frequency regime. The experimental data of LC-AU2 (black squares), LC-ITO (blue circles), and eq 9 (red dotted line) are also shown. Note that the best agreement between the experimental data and the theoretical model is obtained for the case eq 9. For the electrolytic cell with LC-Au, we used $D \approx 5.3 \times 10^{-12} \text{ m}^2 \text{ s}^{-1}$, $\lambda \approx 6.9 \times 10^{-8} \text{ m}$, $\epsilon \approx 7.0\epsilon_0$, $S = 10^{-4} \text{ m}^2$, $d = 36 \times 10^{-6} \text{ m}$, $\bar{\kappa}_1 = 1.17 \times 10^{-7} \text{ m s}^{-1+\delta_1}$, $\delta_1 = 0.55$, $\delta_2 = \delta_1/2$, and $\bar{\kappa}_2 = 1.05 \times 10^{-7} \text{ m s}^{-1+\delta_2}$. For the case with LC-ITO, we used $D \approx 1.6 \times 10^{-11} \text{ m}^2 \text{ s}^{-1}$, $\lambda \approx 1.2 \times 10^{-7} \text{ m}$, $\epsilon \approx 9.0\epsilon_0$, $S = 10^{-4} \text{ m}^2$, $d = 37 \times 10^{-6} \text{ m}$, $\bar{\kappa}_1 = 5.4 \times 10^{-9} \text{ m s}^{-1+\delta_1}$, and $\delta_1 = 0.66$.

details about the procedure used to obtain the experimental data for the Milli-Q and KClO_3 solution can be found in refs 17, 18. The procedure used to obtain the experimental data for the electrolytic cells with LCs is described in ref 19.

The previous discussion shows that the experimental scenarios considered here in the low-frequency regime are suitably described by the PNP model with boundary conditions given by eq 2, and, consequently, it reflects the ionic motion in these electrolytic cells. This point may be better understood by using the electrical conductivity to show the influence of bulk and surface on the ionic motion in this frequency range. The electrical conductivity may be related to the mean square displacement, which is a measure of the ionic motion in the electrolytic cell and consequently gives information about the diffusion occurring in the electrolytic cells. According to the developments described in ref 9, we use eq 10 (see Appendix) in the definition $\sigma = dR/(S|Z|^2)$ to obtain the behavior of the electrical conductivity in the asymptotic limit of low frequency, which is the scenario in which the diffusion and surface effects have a pronounced influence on the electrical response. For the case shown in Figure 2b, after some calculations, it is possible to show that the conductivity, in the low frequency limit, can be approximated to

$$\sigma \approx \bar{\sigma}_1 + \bar{\sigma}_2 \omega^{\delta_2} \quad (3)$$

with $\bar{\sigma}_1 = (\bar{\kappa}_1/\lambda)\Xi_1 C$ and $\bar{\sigma}_2 = (\bar{\kappa}_2/\lambda)\Xi_2 C \cos(\pi\delta_2/2)$, where $\Xi_1 = (1 + (\bar{\kappa}_1/\lambda)\mathcal{R}C)/\Delta$, $\Xi_2 = [1 + 2(\bar{\kappa}_1/\lambda)\mathcal{R}C]/\Delta$, and $\Delta = [1 + (\bar{\kappa}_1/\lambda)\mathcal{R}C(1 + (\bar{\kappa}_1/\lambda)\mathcal{R}C)]$. The effect of the surface on conductivity is evident due to the presence of $\bar{\kappa}_1$ and $\bar{\kappa}_2$ in $\bar{\sigma}_1$ and $\bar{\sigma}_2$. By applying the procedure described in ref 9, it is possible to associate the conductivity given by eq 3 with the mean square displacement. In particular, we can show that

$$\langle(\Delta z)^2\rangle \approx 2d\bar{\kappa}_1\Xi_1 t + \frac{2d\bar{\kappa}_2}{\Gamma(2 - \delta_2)}\Xi_2 t^{1-\delta_2} \quad (4)$$

Equation 4 shows that the ionic motion in the low-frequency limit manifests an interplay between two different regimes with the crossover defined by the characteristic time, $\tau_c \approx \{\bar{\kappa}_2\Xi_2/[\Gamma(2 - \delta_2)\bar{\kappa}_1\Xi_1]\}^{1/\delta_2}$. This behavior reflects the influence of the surfaces and evidences that the waiting time distribution related to the ionic motion for $t \ll \tau_c$ is characterized by a power law (subdiffusion) and for $t \gg \tau_c$ an exponential behavior is exhibited (usual diffusion). For the electrolytic cell with LCs, the behavior of the conductivity is given by

$$\sigma \approx \tilde{\sigma}_1 \omega^{\delta_1} + \tilde{\sigma}_2 \omega^{\delta_2} \quad (5)$$

for the case LC-AU2, and

$$\sigma \approx \tilde{\sigma}_1 \omega^{\delta_1} \quad (6)$$

for the other case LC-ITO. In both cases, we have $\tilde{\sigma}_1 = [(\bar{\kappa}_1/\lambda_D)C] \cos(\pi\delta_1/2)$ and $\tilde{\sigma}_2 = [(\bar{\kappa}_2/\lambda_D)C] \cos(\pi\delta_2/2)$. Similarly to the previous case, we may use the approach presented in ref 9 and connect eqs 5 and 6 with their mean square displacements, yielding

$$\langle(\Delta z)^2\rangle \approx \frac{2d\bar{\kappa}_1}{\Gamma(2 - \delta_1)}t^{1-\delta_1} + \frac{2d\bar{\kappa}_2}{\Gamma(2 - \delta_2)}t^{1-\delta_2} \quad (7)$$

where $0 < \delta_1 < 1$ and $0 < \delta_2 < 1$ for the case LC-AU2, and

$$\langle(\Delta z)^2\rangle \approx \frac{2d\bar{\kappa}_1}{\Gamma(2 - \delta_1)}t^{1-\delta_1} \quad (8)$$

for the case LC-ITO. Equation 7 shows that two different regimes are present in the limit of low frequency for the sample of LC-AU2 with the crossover time, $\tau_{c,AU2} \approx \{(\bar{\kappa}_2/\bar{\kappa}_1)[\Gamma(2 - \delta_1)/\Gamma(2 - \delta_2)]\}^{1/(\delta_2 - \delta_1)}$, indicating that for $t \ll \tau_{c,AU2}$ the diffusion is governed by δ_1 , whereas for $t \gg \tau_{c,AU2}$ the diffusion characterized by δ_2 governs the system, with $\delta_1 < \delta_2$. In this case, the random walk may present a waiting time distribution characterized by two power laws, one of them for $t \ll \tau_{c,AU2}$ and the other one for $t \gg \tau_{c,AU2}$. For the case LC-ITO, we have an anomalous diffusion with $0 < \delta_1 < 1$, and, consequently, the random walk has the waiting time distribution governed by a power law.

CONCLUSIONS

To sum up, we have investigated the diffusive regimes manifested by the ionic motion in an electrolytic cell by considering Milli-Q water, a weak electrolytic solution of KClO_3 , and LCs. In these cases, we first verified, in the low-frequency limit, that the imaginary part of the electrical impedance response of the system presented an imperfect capacitive behavior, that is, $Z \sim 1/(i\omega)^\gamma$, which may be due to a charge accumulation and/or an adsorption-desorption on

the electrode surfaces. The other behaviors exhibited in this limit depend on the substance considered. An evidence of charge transfer between the electrode and the electrolyte was observed, from the experimental data for the Milli-Q water and KClO₃ solution, leading us to consider $\delta_1 = 0$. These effects together indicate that in the low-frequency limit the conductivity is governed by eq 3, which may be related to the ionic motion characterized by eq 4. This equation in turn shows the presence of two different diffusive regimes, one usual and the other anomalous, with a crossover time between them. Thus, the random process related to the ionic motion can be characterized by a waiting time distribution with two different regimes, for example, a power law for $t \ll \tau_c$ and an exponential for $t \gg \tau_c$. We note in this case the presence of relaxation time $\mathcal{R}C$ in $\bar{\sigma}_1$ and $\bar{\sigma}_2$ because of the charge transfer between the electrode and the bulk. This constant is absent in eqs 7 and 8 obtained for the LC systems, for which the charge transfer between the electrode and the bulk is not evidenced by the experimental data as in the previous case. Consequently, different behaviors are found, and in both cases (LC-AU2 and LC-ITO), the random process related to the ionic motion in these samples may be characterized by a waiting time distribution governed by power laws, which are generally related to the behavior of the mean square displacement.²⁷ In all of the cases analyzed here, we observe that the surfaces play an important role in the ionic motion, thus producing an usual or an anomalous diffusion depending on the interaction between electrodes and bulk. It has been shown before that models using boundary conditions of the form of eq 2 embody the effects produced by a constant-phase element (CPE) in an equivalent electrical circuit if an appropriate term in the boundary condition is considered. This result, established on analytical grounds, opens the perspective to describe the low-frequency response data regarding very intricate and different electrolyte systems.¹⁶ Indeed, the formulation based on the fractional diffusion equations establishes on general theoretical grounds a connection between these anomalous diffusion models with an entire framework of continuum models and equivalent circuits with CPEs to analyze the impedance data.¹⁵ Furthermore, in the cases analyzed here, the crossover time between the diffusive regimes is directly influenced by $\bar{\kappa}_1$ and $\bar{\kappa}_2$. This evidences that the parameters associated to the surface processes determine the permanence of the system in these diffusive regimes.

APPENDIX

It is possible to consider a linear approximation for the PNP model subjected to eq 2 when the system is subjected to a periodic applied potential with a very small amplitude. This corresponds to the AC small-signal limit and produces a linear response of the system.²⁶ Under this assumption and after some calculations, we obtain the following expression for the impedance^{19,28}

$$Z = \frac{2}{i\omega\epsilon S a^2} \times \frac{\tanh(ad/2)/(\lambda^2\alpha) + \mathcal{E}d/(2D)}{1 + \bar{\kappa}(i\omega)(1 + i\psi) \tanh(ad/2)/(i\omega\lambda^2)} \quad (9)$$

where $\mathcal{E} = i\omega + \alpha \tanh(ad/2)\bar{\kappa}(i\omega)$, $\alpha^2 = 1/\lambda^2 + i\omega/D$, S is the electrode area, $\bar{\kappa}(i\omega) = e^{-i\omega t} \int_0^1 d\bar{\delta}(i\omega)^{\bar{\delta}} \int_{-\infty}^t \kappa(t - t', \bar{\delta}) e^{i\omega t'} dt'$, $\psi = \omega/\omega_D$, and $\omega_D = D/\lambda^2$, with $\lambda = \sqrt{ek_B T/(2Nq^2)}$ representing the Debye screening length. Equation 9 in the asymptotic limit of low frequency becomes

$$Z \approx \frac{1}{i\omega C + [\bar{\kappa}(i\omega)/\lambda]C} + \mathcal{R} \quad (10)$$

where $C = \epsilon S/(2\lambda)$ and $\mathcal{R} = \lambda^2 d/(\epsilon S D)$. The real part of eq 10 can be related to bulk effects. The imaginary part exhibits a dependence on $\bar{\kappa}(i\omega)$ and consequently shows how the surface influences the system in the low-frequency limit. By a suitable choice of $\bar{\kappa}(i\omega)$, the impedance predicted by this model is able to reproduce the experimental data.

AUTHOR INFORMATION

Corresponding Author

*E-mail: lre@dfi.uem.br. Phone: +55 44 3011 6039. Fax: +55 44 3263 4623.

ORCID

L. R. Evangelista: 0000-0001-7202-1386

Notes

The authors declare no competing financial interest.

ACKNOWLEDGMENTS

This work was partially supported by the National Institute of Science and Technology for Complex Systems (INCT-SC, Rio de Janeiro, Brazil) and the National Institute of Science and Technology of Complex Fluids (INCT-Fcx, São Paulo, Brazil).

REFERENCES

- (1) Einstein, A. Über die von der molekularkinetischen Theorie der Wärme geforderte Bewegung von in ruhenden Flüssigkeiten suspendierten Teilchen. *Ann. Phys.* **1905**, *322*, 549–560.
- (2) von Smoluchowski, M. Zur kinetischen Theorie der Brownschen Molekularbewegung und der Suspensionen. *Ann. Phys.* **1906**, *326*, 756–780.
- (3) Langevin, P. Sur la théorie du mouvement brownien. *C. R. Acad. Sci.* **1908**, *146*, 530–533.
- (4) Barkai, E.; Garini, Y.; Metzler, R. Strange kinetics of single molecules in living cells. *Phys. Today* **2012**, *65*, 29–35.
- (5) Ghosh, S. K.; Cherstvy, A. G.; Grebenkov, D. S.; Metzler, R. Anomalous, non-Gaussian tracer diffusion in crowded two-dimensional environments. *New J. Phys.* **2016**, *18*, No. 013027.
- (6) Coquel, A.-S.; Jacob, J.-P.; Primet, M.; Demarez, A.; Dimiccoli, M.; Julou, T.; Moisan, L.; Lindner, A. B.; Berry, H. Localization of protein aggregation in *Escherichia coli* is governed by diffusion and nucleoid macromolecular crowding effect. *PLoS Comput. Biol.* **2013**, *9*, No. e1003038.
- (7) Scher, H.; Montroll, E. W. Anomalous transit-time dispersion in amorphous solids. *Phys. Rev. B* **1975**, *12*, 2455–2477.
- (8) Sidebottom, D. L. Colloquium: Understanding ion motion in disordered solids from impedance spectroscopy scaling. *Rev. Mod. Phys.* **2009**, *81*, 999–1014.
- (9) Scher, H.; Lax, M. Stochastic transport in a disordered solid. I. Theory. *Phys. Rev. B* **1973**, *7*, 4491–4502.
- (10) Scher, H.; Lax, M. Stochastic transport in a disordered solid. II. Impurity conduction. *Phys. Rev. B* **1973**, *7*, 4502–4519.
- (11) Singh, M. B.; Kant, R. Theory for anomalous electric double-layer dynamics in ionic liquids. *J. Electroanal. Chem.* **2013**, *704*, 197–207.
- (12) Tadapatri, P.; Krishnamurthy, K. S.; Weissflog, W. Multiple electroconvection scenarios in a bent-core nematic liquid crystal. *Phys. Rev. E: Stat., Nonlinear, Soft Matter Phys.* **2010**, *82*, No. 031706.
- (13) Kaur, S.; Belaissaoui, A.; Goodby, J. W.; Gortz, V.; Gleeson, H. F. Nonstandard electroconvection in a bent-core oxadiazole material. *Phys. Rev. E: Stat., Nonlinear, Soft Matter Phys.* **2011**, *83*, No. 041704.
- (14) Wiant, D.; Gleeson, J. T.; Éber, N.; Fodor-Csorba, K.; Já, A.; Tóth-Katona, T. Nonstandard electroconvection in a bent-core nematic liquid crystal. *Phys. Rev. E: Stat., Nonlinear, Soft Matter Phys.* **2005**, *72*, No. 041712.

(15) Lenzi, E. K.; Lenzi, M. K.; Silva, F. R. G. B.; Gonçalves, G.; Rossato, R.; Zola, R. S.; Evangelista, L. R. A framework to investigate the immittance responses for finite length-situations: Fractional diffusion equation, reaction term, and boundary conditions. *J. Electroanal. Chem.* **2014**, *712*, 82–88.

(16) Lenzi, E. K.; de Paula, J. L.; Silva, F. R. G. B.; Evangelista, L. R. A connection between anomalous Poisson–Nernst–Planck model and equivalent circuits with constant phase elements. *J. Phys. Chem. C* **2013**, *117*, 23685–23690.

(17) Silva, F. R. G. B.; Ribeiro, H. V.; Lenzi, M. K.; Petrucci, T.; Michels, F. S.; Lenzi, E. K. Fractional diffusion equations and equivalent circuits applied to ionic solutions. *Int. J. Electrochem. Sci.* **2014**, *9*, 1892–1901.

(18) Lenzi, E. K.; Fernandes, P. R. G.; Petrucci, T.; Mukai, H.; Ribeiro, H. V.; Lenzi, M. K.; Gonçalves, G. Anomalous diffusion and electrical response of ionic solutions. *Int. J. Electrochem. Sci.* **2013**, *8*, 2849–2862.

(19) Ciuchi, F.; Mazzulla, A.; Scaramuzza, N.; Lenzi, E. K.; Evangelista, L. R. Fractional diffusion equation and the electrical impedance: Experimental evidence in liquid-crystalline cells. *J. Phys. Chem. C* **2012**, *116*, 8773–8777.

(20) Lenzi, E. K.; Zola, R. S.; Rossato, R.; Ribeiro, H. V.; Vieira, D. S.; Evangelista, L. R. Asymptotic behaviors of the Poisson–Nernst–Planck model, generalizations and best adjust of experimental data. *Electrochim. Acta* **2017**, *226*, 40–45.

(21) Chang, H.; Jaffe, G. Polarization in electrolytic solutions. Part I. Theory. *J. Chem. Phys.* **1952**, *20*, 1071–1077.

(22) Lenzi, E. K.; Evangelista, L. R.; Barbero, G.; Mantegazza, F. Anomalous diffusion and the adsorption-desorption process in anisotropic media. *Europhys. Lett.* **2009**, *85*, No. 28004.

(23) Lenzi, E. K.; Yednak, C. A. R.; Evangelista, L. R. Non-Markovian diffusion and the adsorption-desorption process. *Phys. Rev. E: Stat., Nonlinear, Soft Matter Phys.* **2010**, *81*, No. 011116.

(24) Guimarães, V. G.; Ribeiro, H. V.; Li, Q.; Evangelista, L. R.; Lenzi, E. K.; Zola, R. S. Unusual diffusing regimes caused by different adsorbing surfaces. *Soft Matter* **2015**, *11*, 1658–1666.

(25) Barbero, G.; Evangelista, L. R. *Adsorption Phenomena and Anchoring Energy in Nematic Liquid Crystal*; Taylor and Francis: London, U.K., 2006.

(26) Macdonald, J. R. Impedance spectroscopy and its use in analyzing the steady-state AC response of solid and liquid electrolytes. *J. Electroanal. Chem.* **1987**, *223*, 25–50.

(27) Metzler, R.; Klafter, J. The random walk's guide to anomalous diffusion: Fractional dynamic approach. *Phys. Rep.* **2000**, *339*, 1–77.

(28) Lenzi, E. K.; Fernandes, P. R. G.; Petrucci, T.; Mukai, H.; Ribeiro, H. V. Anomalous-diffusion approach applied to the electrical response of water. *Phys. Rev. E: Stat., Nonlinear, Soft Matter Phys.* **2011**, *84*, No. 041128.